Journal of Applied Polymer Science

The effect of wood-fiber type on the thermomechanical performance of a biodegradable polymer matrix

Panayiotis Georgiopoulos, Evagelia Kontou
Department of Applied Mathematical and Physical Sciences, Section of Mechanics, National Technical University of Athens, GR-15773, Athens, Greece
Correspondence to: E. Kontou (E-mail: ekontou@central.ntua.gr)

ABSTRACT: The effect of type and content of wood fibers on the thermal, mechanical and rheological behavior of the commercial biodegradable polyester product, Ecovio® (BASF) is analytically studied. Ecovio® is basically a blend of poly(butylene adipate-terephthalate) copolyester (Ecoflex®, BASF) and polylactide. Three different types of wood fibers, based either on raw cellulose (Arbocel) or selected conifers (Lignocel), with varying fiber size at various weight fractions were used for this purpose. The role of these fibers on the thermomechanical performance of Ecovio® was investigated in terms of several experimental techniques including scanning electron microscopy, differential scanning calorimetry, dynamic mechanical analysis, creep, tensile testing, and water uptake at room temperature. At the low wood fiber content (20 wt %), Lignocel composite's properties are predominant compared with the Arbocel composites. It has been found, that at this wood content, an efficient compatibility between matrix and fibers is achieved, leading to superior reinforcement. This trend is completely reversed at higher filler loading, probably due to the poor interfacial adhesion between the matrix and Lignocel occurring at 30 wt %. This behavior was supported by all the experimental methods employed. © 2015 Wiley Periodicals, Inc. J. Appl. Polym. Sci. **2015**, *132*, 42185.

KEYWORDS: biodegradable; cellulose and other wood products; composites; mechanical properties

Received 12 November 2014; accepted 9 March 2015
DOI: 10.1002/app.42185

INTRODUCTION

Biobased polymers made from renewable resources have been found as a potential replacement to resolve the environmental issues associated with petroleum-based polymers, while they are connected with a variety of biomedical, structural, electrical applications and food packaging or agriculture. These biodegradable polymers are mainly the aliphatic polyesters produced by microbiological and chemical synthesis, natural polymer-based products, and their blends.[1–3] Among them, poly(lactic acid) (PLA), polycaprolactone (PCL), polybutylenesuccinate (PBS), and polybutylensuccinate–butylenecarbonate (PBSC) are commercially available at present.[4]

Polylactide (PLA) is a thermoplastic material, belonging to the family of environmentally friendly biodegradable polymers which has attracted a lot of attention in recent years.[5,6] Poly(butylene adipate-*co*-terphthalate) (PBAT) is a biodegradable fossil-based aliphatic-aromatic copolyester.[7]

Blends of a soft polyester like PBAT and a high-stiffness polymer like PLA were used to achieve specific mechanical properties by making flexible materials with reduced stiffness by adding PBAT or *vice versa*.[8]

The thermal and mechanical resistance of these materials can be improved by the addition of nanosized or microsized fillers or a combination of them, consisting simple and economic ways for producing a desirable material with specific properties.[9,10]

Study of a new material system, based on the commercialized PBAT/PLA blend, Ecovio® produced by BASF and consisted by 45% of renewable resources has been performed in Ref. [11. Two different filler types namely silica nanoparticles and wood fibers were employed for the mechanical enhancement of Ecovio®. A comparative study of the thermomechanical properties between the two series of composites, was performed to detect the different matrix-filler interactions.

The incorporation of lignocellulosic material as a filler into polymer composites has received increased attention particularly for price driven and high volume applications. The advantages of natural fiber composites are their low density, low cost, renewable characteristics, and complete biodegradability.[12]

Wood/plastic composites (WPCs) have attracted attention in this context, because WPCs are regarded as an effective means of using waste wood and/or plastic.[13] Furthermore, wood acquires one of the important characteristics of plastic, that of

Table I. Material Types Examined

Abbreviation	Wood flour type	Filler content (wt) (%)	Grain size (μm)
EC	-	0	-
ECLWF20	Lignocel BK 40-90	20	300-500
ECLWF30	Lignocel BK 40-90	30	300-500
ECAWF20	Arbocel C320	20	200-500
ECAWF30	Arbocel C320	30	200-500
ECBWF20	Arbocel C100	20	70-150
ECBWF30	Arbocel C100	30	70-150

easy molding, in WPCs.[13,14] When hydrophilic wood and hydrophobic plastic are mixed,[13] their interfacial adhesion is not good because of their poor compatibility, leading to poor mechanical properties of the composite. To improve their compatibility, various compounds have been tested and reported so far; in general, a small amount of polyolefin modified with maleic anhydride (MAPO) was found to be an effective compatibilizer, and many kinds of maleic anhydride-modified polyethylene (MAPE) or polypropylene (MAPP) are now commercially available.[13] Marcovich *et al.*[15] studied the effect of chemically modified wood flour on the properties of composites using unsaturated polyester as the plastic. They found that composites prepared with maleic anhydride-treated wood flour had better performance under compressive loads. These results suggest that derivatives of natural products might be promising compatibilizers of WPCs.

The use of wood flour (WF) can reduce material costs and provide specific properties such as low density, high specific stiffness, and biodegradability.[16–19] In particular, WPCs with 50 wt % or less polymer by weight, have been accepted by the construction industry and homeowners, largely for decking, fencing, roofing, window profile, and automotives.[17] Talc (up to 30% by weight) can have a positive influence on modulus, strength, processing efficiency, creep and elastic recovery performance of WPCs.[20] A combination of organic (e.g., wood) and inorganic (e.g., talc) fillers in PLA may lead to interesting composite properties. The effects of WF and talc loading with silane treatment on thermal, mechanical, and morphological properties of the PLA-based composites were thoroughly studied in Ref. [16. Thermogravimetric analysis (TGA), differential scanning calorimetry (DSC), scanning electron microscopy (SEM), and stress–strain behavior were employed to evaluate the thermal degradation, thermal transition, morphological, and mechanical properties of the composites.[16] In recent years, several studies have been made for the use of wood fibers as a reinforcement for biodegradable polymers,[4,21–26] introducing a different potential for wood composites.

In the present study, a new material system, based on PBAT/PLA blend, Ecovio®, reinforced by three different types of wood fibers is examined. The aim of this work is the experimental study of the effect of various types of wood fibers on the thermomechanical performance and viscoelastic properties of Ecovio®. Given that the relative humidity is a crucial factor affecting the materials macroscopic behavior, the water uptake of the composites under examination has also been measured.

EXPERIMENTAL

Materials

The selected grade Ecovio® L BX 8145 (EC) is basically a blend of poly(butylene adipate-terephthalate) (PBAT) copolyester (Ecoflex® F BX 7011), which is based on nonrenewable resources, and PLA (NatureWorks). Because of the PLA content, Ecovio® L BX 8145 consists of 45% of renewable resources. The material in pellets form was dried at 75°C for a minimum of 4 h prior to use in a desiccating dryer. Melt mixing of wood fibers with the matrix was performed with a Brabender mixer at a temperature of 180°C, while the rotation speed of the screws was 40 rpm. Maleic anhydrite was used at 2 wt % content, as well as dicumil peroxide 0.7 wt %, to enhance compatibilty between wood and the polymer. In Ref. [27, a detailed analysis concerning the effect of reactive modifier, initiator, and processing conditions on the final grafted maleic anhydride of PLA is presented.

The temperature for melt-mixing was kept as low as possible in order to minimize the effect of degradation. Hereafter, the material was compression molded at 130°C, using a thermopress and a special mould of 1 mm thickness. The material was then cooled slowly down at ambient temperature. Three different wood-fiber (or wood-flour) types, were used at a content of 20 and 30 wt % each, in order to prepare 6 different composite materials. The first wood fiber was of type Lignocel® BK 40/90, which is cubic structured soft wood from selected conifers with a particle size between 300 and 500 μm. The second type designated as Arbocel® C-320 and the third type Arbocel® C-100, are raw cellulose fibers with a particle size 200 to 500 μm and 70 to 150 μm correspondingly. Wood flour was kindly supplied by J. Rettenmaier & Sohne, Rosenberg, Germany. All materials types and their abbreviations are presented in Table I.

Fourier Transform-Infrared Spectroscopy (FT-IR)

FT-IR measurements were made by using a Bruker Equinox 55 spectrometer. Sixty-four scans were collected for each spectrum at 2 cm^{-1} resolution.

Scanning Electron Microscopy

Scanning electron microscopy (SEM) images were obtained by direct observation of the topography of the sample's surface with a Nova™ NanoSEM 230 (FEI, Hillsboro, OR) scanning microscope operated at acceleration voltage of 5 either 15 kV. All the studied samples were coated with gold to avoid charging under the electron beam.

Differential Scanning Calorimetry

Calorimetric measurements (DSC) were carried out using a Setaram DSC 141 instrument, calibrated with an Indium standard. Each sample was heated at a constant heating rate of 5°C/min from 20 up to 180°C, and the thermogram was recorded. DSC samples were taken from the centre and the edge of a 2-mm-thick material sheet. Three specimens of each sample were measured and the results were averaged and summarized in Table I.

Table I. IDSC Results

Material	T_g (°C)	T_{cc} (°C)	T_{m1} (°C)	T_{m2} (°C)	ΔH_r (J/g)	ΔH_{cc} (J/g)	ΔH_m (J/g)	ΔH^a (J/g)
EC	60.3	109.5	146.3	150.5	1.9	−2.9	8.6	5.6
ECLWF20	59.7	98.8	144.5	151.2	1.5	−2.8	8.4	6.8
ECLWF30	59.4	98.9	144.3	152.2	1.6	−5.0	8.1	4.1
ECAWF20	59.8	106.8	145.6	149.7	1.4	−1.8	6.9	6.2
ECAWF30	59.4	104.3	145.9	150.3	1.0	−1.2	7.3	8.0
ECBWF20	59.4	102.1	146.8	150.6	1.5	−0.8	7.1	7.6
ECBWF30	59.1	100.6	145.4	151	1.0	−0.7	7.0	8.2

[a] Enthalpy values normalized to pure polymer.

Tensile Experiments

Tensile measurements were performed at room temperature, following the procedure presented in Ref. [28. Five specimens of pristine Ecovio® and of each composite were tested, and the average scatter is presented in Table III.

Dynamic Mechanical Analysis

Dynamic mechanical analysis (DMA) experiments were performed using the TA Instruments DMA Q800 instrument. The mode of deformation applied was the single cantilever beam, and the mean dimensions of sample plaques were 12.6 mm × 2 mm × 17.5 mm. The temperature range varied from 25 up to 120°C. The temperature dependent behavior was studied by monitoring changes in force and phase angle, keeping the amplitude of oscillation constant. The experiments were performed at five frequency values of 1, 5, 10, 20, and 40 Hz, and the heating rate was 3°C/min. The storage and loss modulus master curves versus temperature were then evaluated, by applying the time–temperature superposition principle.

Creep Experiments

Tensile creep experiments have also been performed with TA Q800, for a specific time period equal to 60 min, at ambient temperature 25°C. Two stress levels namely 2.5 and 4.5 MPa have been applied for the tensile creep tests, for all material types.

Water Uptake Experiments

Water absorption was determined according to ASTM D570 method. After drying for 24 h, the weight and the thickness of the samples were measured. Then, they were immersed in distilled water at room temperature. Each sample was removed from the water, dried by wiping with blotting paper and weighed immediately in order to calculate the water uptake. Moreover, the thickness of each sample was measured in order to determine the thickness swelling. After each measurement, the samples were immersed in the water again.

RESULTS AND DISCUSSION

Fourier Transform-Infrared Spectroscopy

In Figure 1, a representative FT-IR spectrum for Ecovio® and ECWF composite, namely ECAWF30, is depicted. From Figure 1, it was not possible to detect a peak related to the grafting of maleic anhydride on matrix. Following Detyothin *et al.*,[27] the peak at 1854 cm^{-1} (C—O stretching) is a weak shoulder, and the same is with the peak at 695 cm^{-1} (CH bending). Both peaks are very weak for PLA, and it is reasonable to assume that they could not be detected in our polymer matrix which is a blend of PLA and PBAT (containing in total only 45 wt % PLA). This effect denotes that the addition of maleic anhydrite had no effect on the FT-IR spectrum of the ECWF composite.

Scanning Electron Microscopy

In Figure 2, representative SEM images of the tensile fracture surfaces of the composites are depicted. The Lignocel composites [Figure 2(a,b)] exhibit a rather rough surface compared with a clearly smoother and more compact surface observed in Arbocel ones [Figure 2(c,d)]. Apart from this, clean fiber surfaces almost separated from the matrix are observed for ECLWF30, indicating poor adhesion between the wood and the matrix. Regarding Arbocel composites, the identification of the wood particles was difficult, especially for ECBWF30, probably due to strong fiber-matrix adhesion. Moreover, for all composites except ECLWF30, a great number of fiber fractures can be seen, while no clear evidence for pulled-out fibers exists. The existence of the broken fibers, indicates that they do not

Table III. Tensile Results

Material	Young's modulus (MPa)	Yield stress (MPa)	Failure stress (MPa)	Failure strain (%)
EC	414 ± 56	13 ± 0.7	17.13 ± 1.1	19.8 ± 1
ECLWF20	1281 ± 59	14.8 ± 0.5	14.8 ± 0.5	3.6 ± 0.7
EC.LWF30	1154 ± 77	14.8 ± 0.6	14.8 ± 0.6	2.6 ± 0.8
ECAWF20	1141 ± 71	15.6 ± 0.4	15.6 ± 0.4	2.7 ± 0.8
ECAWF30	1313 ± 81	18 ± 0.4	18 ± 0.4	4.7 ± 1
ECBWF20	1173 ± 65	16.1 ± 0.4	16.1 ± 0.4	2.6 ±0.9
ECBWF30	1480 ± 106	16.7 ± 0.5	16.7 ± 0.5	4.1 ± 0.6

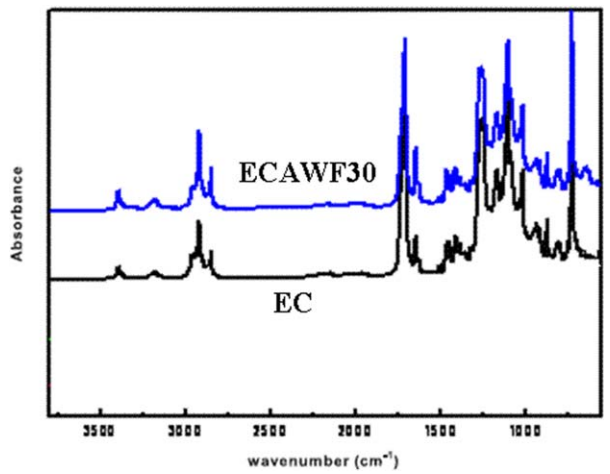

Figure 1. FT-IR spectra of EC and ECAWF30. [Color figure can be viewed in the online issue, which is available at wileyonlinelibrary.com.]

separate from the matrix before fracture, due to strong adhesion between them. At ECLWF30, an agglomeration seems to exist but generally they cannot be clearly identified.

Differential Scanning Calorimetry

The DSC results of pristine Ecovio® (EC) and its composites, presented in Figure 3 and summarized in Table I, show three transitions. A glass transition temperature T_g, expressed by an endothermic peak is obtained, followed by a cold crystallization temperature and a melting region hereafter. According to these results, the T_gs of the ECWF composites are almost equal to the T_g of the pristine Ecovio®; i.e., in all series of the composites examined, the filler type and content variation do not affect the T_g. The experimental fact that the T_g of the ECWF composites is not further affected by the filler content and type is similar to the one observed in Ref. [11, for both EC/nanocomposites and EC/composites. Moreover, the relaxation enthalpy ΔH_r (normalized to the weight of pure polymer) at the T_g region is decreased for all EC/composites, with the ECWFL composites exhibiting the lowest ΔH_r decrement. The ΔH_r decrement implies a confinement of some fraction of polymeric chains around the fillers' surface (interface) which cannot contribute to enthalpy relaxation.[29] In addition, the relaxation enthalpy at the T_g is related to the melting of a mesophase with certain molecular ordering.[30] From the results of Table I it is extracted that the mesophase formation is favored

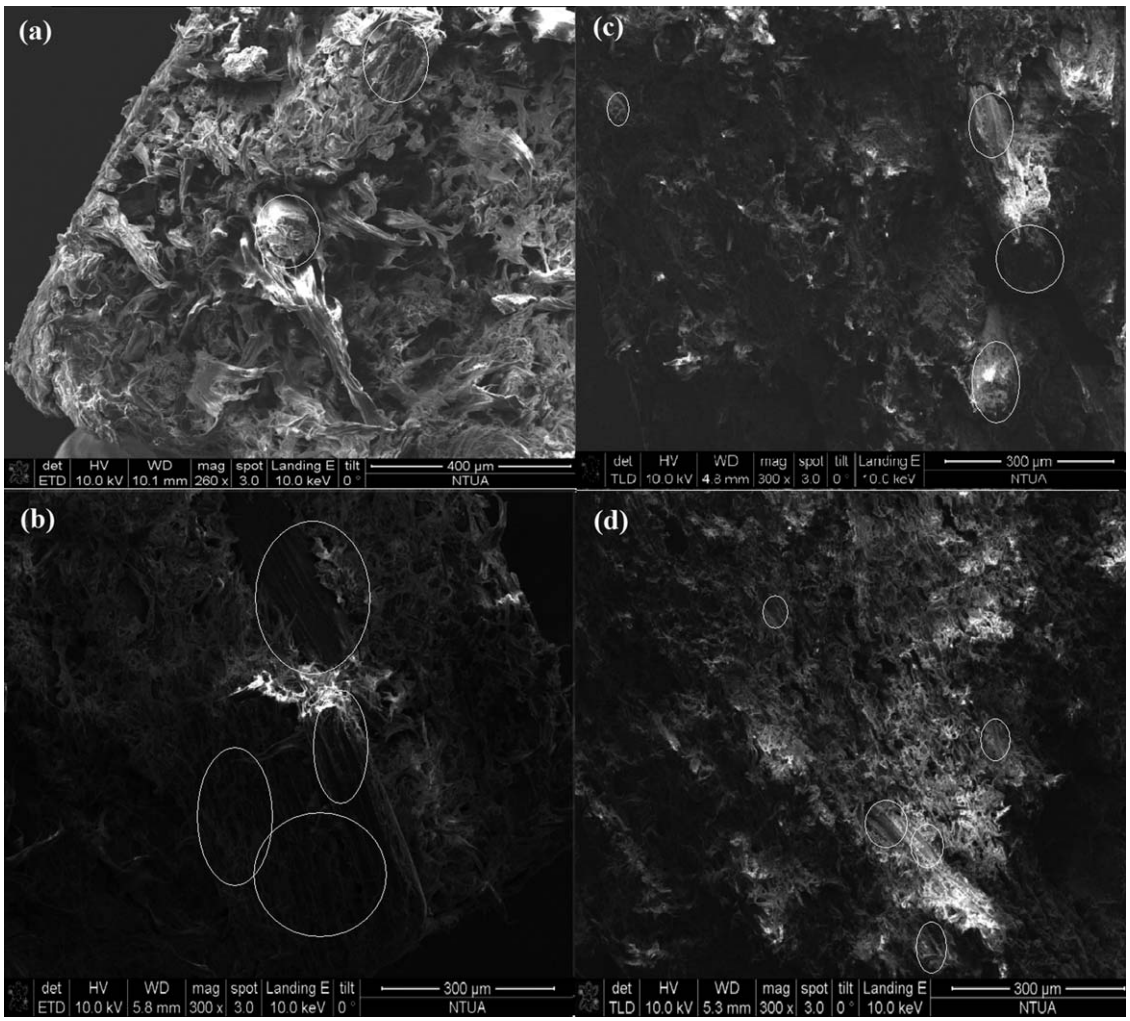

Figure 2. SEM micrograph of (a) ECLWF20, (b) ECLWF30, (c) ECAWF30, (d) ECBWF30.

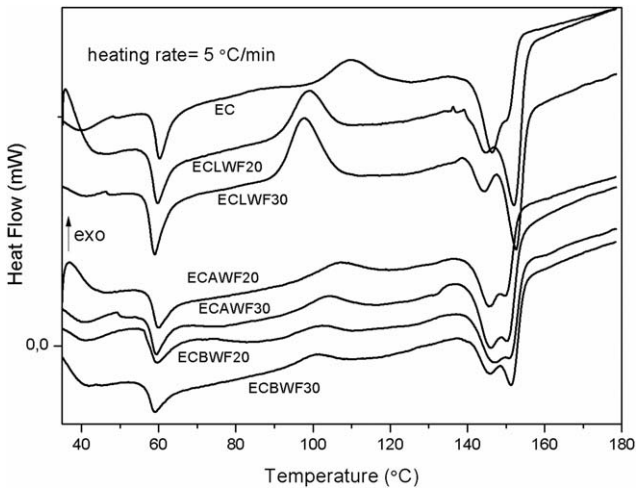

Figure 3. DSC thermograms of pristine EC and EC composites.

in the case of Arbocel type wood fibers, probably due to the smaller average filler size.

Analyzing further the results of Table I and Figure 3, a cold crystallization temperature (T_{cc}) is noticed in pristine Ecovio® (at 109.5°C), while this temperature is lowered for ECWF composites. The ECLWF20 and ECLWF30 composites display a sharp cold crystallization peak and a higher area of this exothermic peak.

ECAWF and ECBWF composites display a broader and smaller cold crystallization area. The lowering of the cold crystallization temperature in respect to pristine Ecovio® indicates that the incorporation of wood fibers considerably promotes kinetics and extent of Ecovio® crystallization on heating, and this effect seems to be enhanced as the fiber length is increased. When cold crystallization occurs, imperfect crystals are formed, which melt during the DSC heating run. The formation of the mesophase seems to be related to the T_{cc} temperature decrement, given that the ECLWF composites demonstrate the highest T_{cc} decrement and the highest relaxation enthalpy ΔH_r compared with the rest of the materials.

Regarding melting region, two melting peaks (T_{m1} and T_{m2}) between 145 and 152°C were observed for all materials examined, with the second peak being more intense for Lignocel composites. T_{m1} is related to the fusion of imperfect crystallites, formed during cold crystallization upon heating, and T_{m2} related to the fusion of new crystallites formed through the melt-recrystallization process.[30] For the EC matrix, T_{m2} appears as a shoulder. The first melting peak T_{m1} is lowered for the ECLWF composites, and this effect is in accordance with the lower cold crystallization temperature of the same sample. The second melting peak remains almost constant, with the ECLWF20 and ECLWF30 exhibiting the highest melting temperature T_{m2} of 152°C. This is in contradiction with previous results, where T_m of pristine Ecovio® does not present any significant change with the presence of fillers.[11] Given that the T_m of PBAT is between 110 and 115°C and the T_m of PLA is around 155°C,[31] it is deduced that the T_m of the matrix is close to that of PLA, which is one of the components of the polymeric matrix. The overall heat of fusion ΔH^*, which is the difference ($\Delta H_m - \Delta H_{cc}$), normalized to the weight of pure polymeric matrix, generally increased for all composites, and therefore crystallinity content increased, in respect to pristine Ecovio® (Table I), with the exception of ECLWF30, meaning that the fillers act as effective nucleating agents. The higher values of the percentage crystallinity increment are exhibited by ECAWF30, ECBWF20, and ECBWF30, revealing that the smaller fiber size leads to increased crystallinity, at the filler content examined.

Tensile Results

The experimental tensile results of pristine Ecovio® and its composites are depicted in Figures 4 and 5 and Table III. In Figures 4 and 5 the tensile results for the ECWF composites at 20 wt % and 30 wt % correspondingly are plotted. The elongation at break, which is 20% for pristine Ecovio®, decreases almost 80% in the ECWF composites; the dramatic decrease of the elongation at break in the ECWF composites is attributed to the high content of wood-flour (20–30%), showing a high resistance to deformation. Similar effect was obtained in Ref. [12, where the ductile behavior of the composites was reduced, as a consequence of the rigid nature of the fibers.

Regarding the reinforcement effect, the Young's modulus increases with wood fiber content, exhibiting the highest increment 220% for ECBWF30. High elastic modulus composites are usually required in several important applications such as in structural materials, and the composites under investigation seem to be favorable to this requirement. The highest Young's modulus increment was obtained for ECLWF20, ECAWF30, and ECBWF30, denoting that 20 wt % is an optimum content for Lignocel fibers and 30 wt % for Arbocel fibers, while the smaller fiber size, the higher Young's modulus.

The yield stress of the composites is always higher than that of the matrix, while the highest yield stress is exhibited by the ECAWF30. Regarding Lignocel composites, yield stress seems not to be affected by the wood-flour content.

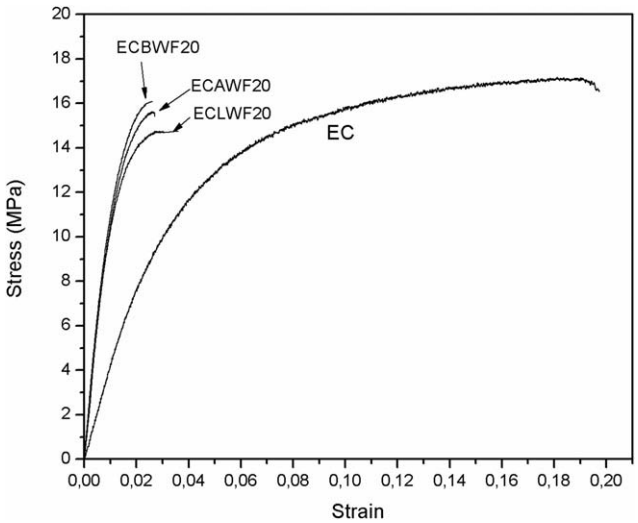

Figure 4. Tensile stress–strain curves of EC and its composites at 20 wt % in wood fibers, at a strain rate 4.16×10^{-4} s^{-1}.

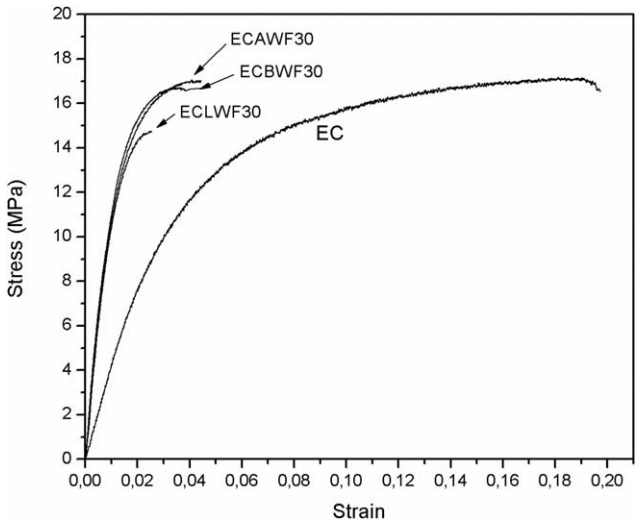

Figure 5. Tensile stress–strain curves of EC and its composites at 30 wt % in wood fibers, at a strain rate 4.16×10^{-4} s^{-1}.

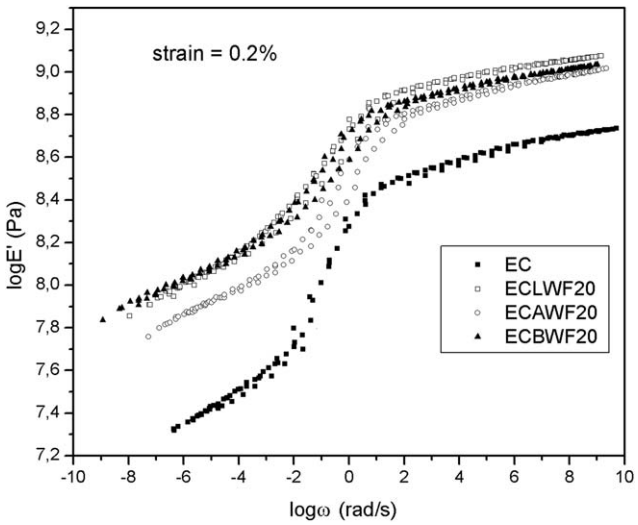

Figure 6. Storage modulus master curves, at a reference temperature 60°C, of EC and its composites at 20 wt % in wood fibers.

The tensile strength, on the other hand, is slightly decreased for the ECWF composites, with the exception of ECAWF30, where it is increased. This slight decrement may be associated with an enhancement of fiber–fiber contact, resulting in an inefficient stress transfer between fibers. Generally, the expected reinforcing effect, among other factors, depends on the interfacial adhesion between matrix and filler, which permits an efficient stress transfer from the two phases. In addition to that, fiber agglomeration which is more intense at high fiber content, as it was noticed in SEM results, leads to stress transfer decrement between the matrix and fiber[12] and not significant tensile strength increment. Moreover, at higher fiber loading, the possibility of microvoid formation is also higher,[32] and this is related to the brittleness of the materials, which after yielding are driven to failure. The fact that the incorporation of filler into thermoplastic matrices does not necessarily increase the tensile strength has also been mentioned in previous studies.[33,34] Comparing the composites with Arbocel fibers, although shorter fibers lead to higher stiffness reinforcement (Table III), the highest tensile strength is achieved for ECAWF30 suggesting that its longer fibers receive the applied load more efficiently, compared with ECBWF composite, at higher stress values.

Dynamic Mechanical Analysis

Following the DMA experimental data, and applying the time-temperature superposition principle (TTS), the corresponding master curves of storage and loss modulus have been constructed, at a reference temperature of 60°C, and are shown in Figures 6 to 9 for all materials examined. Since the curves overlap in the frequency range examined, a thermorheologically simple behavior can be assumed.[35,36] The fact that the loss modulus master curves were constructed with the same shift factor values used for the storage modulus master curves consist another evidence that the implementation of TTS principle is valid.[37]

Regarding storage modulus E' (Figures 6 and 7), the systematic reinforcing effect with increasing filler content, for all material types, is exhibited, due to the increment of structural rigidity caused by the presence of wood fibers. Moreover, the height distance of storage modulus between the rubbery and glassy state plateau is decreased for the composites, especially for 30 wt % in wood fibers, compared with that of pristine Ecovio®. This effect reveals the appearance of a more solid like behavior. The observed enhancement of storage modulus at low frequencies is much more intense than that in high frequencies. This is an indication of the presence of local structures and do not represent a space-filling filler network.[38] The presence of strong local structures leads to a weaker frequency dependence in the low frequency range. Polymeric chains are absorbed on the particle's surface resulting in a transient filler-polymer network and slow dynamics of the bound polymer.

The loss modulus peak (Figures 8 and 9) increases with increasing filler loading. This effect may be attributed to the formation

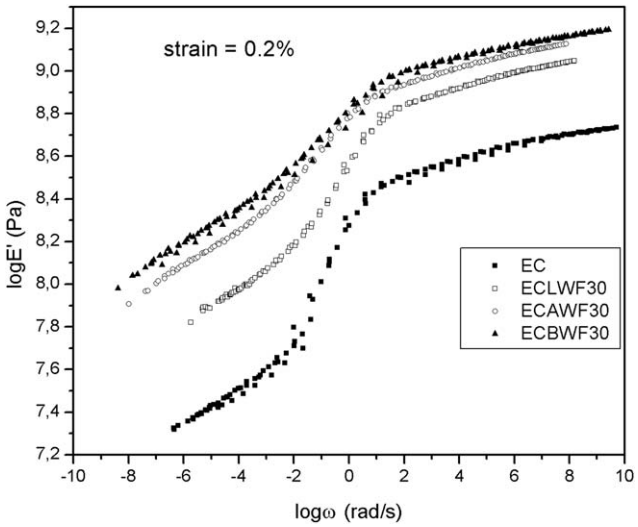

Figure 7. Storage modulus master curves, at a reference temperature 60°C, of EC and its composites at 30 wt % in wood fibers.

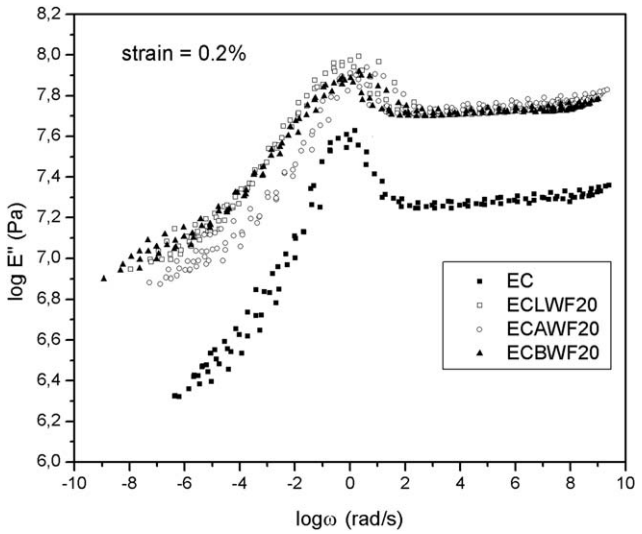

Figure 8. Loss modulus master curves, at a reference temperature 60°C, of EC and its composites at 20 wt % in wood fibers.

of a physical network between the fillers, which can act as a mechanism of energy dissipation, indicating that the composites have greater resistance to flow under a stress field at T_g. Moreover, a loss modulus peak broadening is observed for the composites, while no substantial shifting of the peak frequency is obtained, compared with the pristine matrix.

Creep

The tensile creep results at the two stress levels examined, for all material types are presented in Figures 10 to 13. In all cases, the creep resistance of the composites is higher than that of the matrix. A decrease of the creep strain with increasing filler loading is obtained, meaning that creep resistance was enhanced by the addition of fillers, revealing this way the solid-like behavior of the composites. More specifically, regarding the different effect of wood fibers, from Figures 10 and 11, it is obtained that for the stress of 2.5 MPa, and WF 20 wt %, ECLWF20

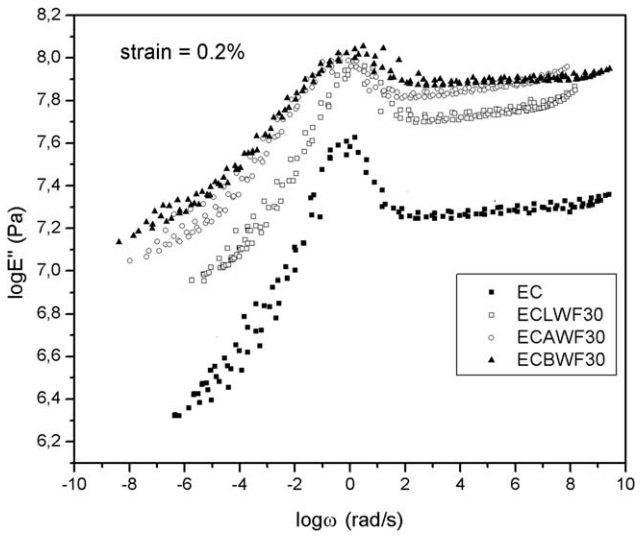

Figure 9. Loss modulus master curves, at a reference temperature 60°C, of EC and its composites at 30 wt % in wood fibers.

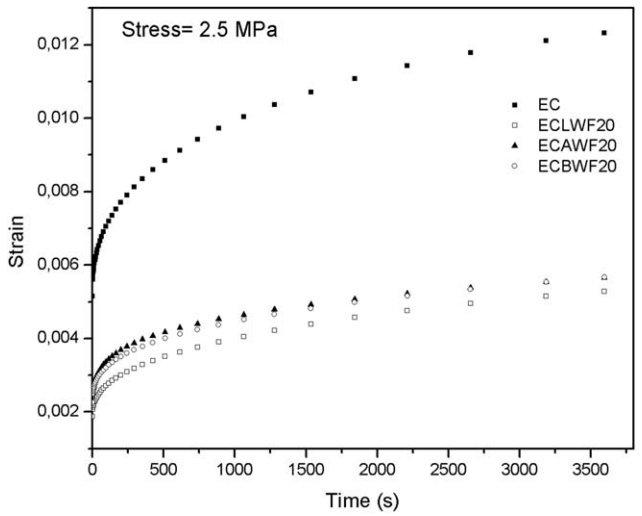

Figure 10. Tensile creep curves at 2.5 MPa of EC and its composites at 20 wt % in wood fibers.

exhibits the lowest creep strain compared with ECAWF30 and ECBWF30, while at WF 30 wt % this trend is reversed. From Figures 12 and 13, it is extracted that at a stress 4.5 MPa, the greater creep resistance is shown by ECBWF20 and ECAWF30 and ECBWF30. Therefore, from the tensile creep results, it can be summarized that generally the raw cellulose fibers Arbocel® C-320 and Arbocel® C-100, have a better effect on the creep resistance of the composites, and this is in accordance with the above-mentioned tensile and DMA results. Moreover, given that Lignocel fibers at 20 wt % provide reinforcement similar to that of Arbocel at higher content, we can conclude that below 30%, there is a sufficient adhesion between the selected conifers and the matrix. Larger fibers seem to allow more efficient stress transfer at this low wood fiber content.

Water Uptake

The water absorption WA and the thickness swelling TS were calculated by eqs. (1) and (2) correspondingly.

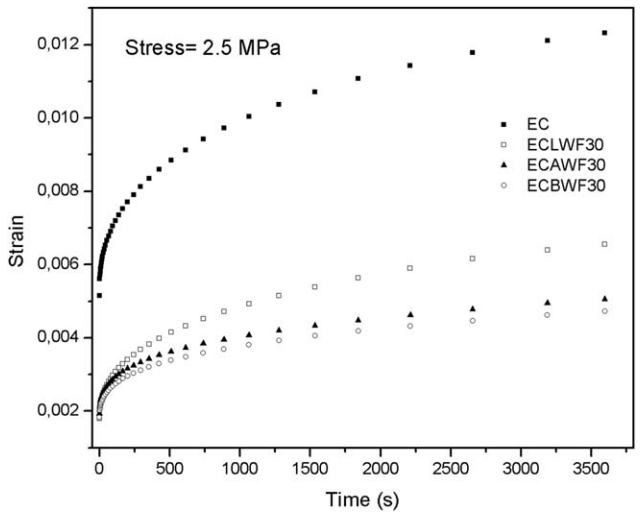

Figure 11. Tensile creep curves at 2.5 MPa of EC and its composites at 30 wt % in wood fibers.

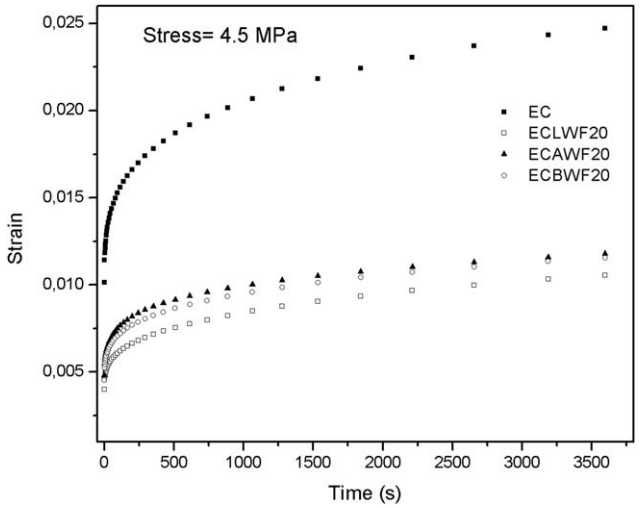

Figure 12. Tensile creep curves at 4.5 MPa of EC and its composites at 20 wt % in wood fibers.

$$\mathrm{WA}(\%) = \frac{M(t) - M_0}{M0} \times 100\% \quad (1)$$

$$\mathrm{TS}(\%) = \frac{d(t) - d_0}{d0} \times 100\% \quad (2)$$

where $M(t)$ and $d(t)$ are the sample weight and the sample thickness correspondingly at time t, and M_0 and d_0 are the initial weight and thickness.

Figures 14 and 15 show the variation of the water absorbance and the thickness swelling correspondingly, for the various wood fiber types and contents versus immersion time. Both quantities increased with wood flour content due to the high hygroscopicity of wood compared with that of the pure polymers. The Ecovio matrix hardly absorbs water in the first day of immersion, while its water uptake after that time seems not to change further. Considering the composites, we observe a rapid water absorbance during the first days of immersion which decreased after 3 to 4 days, reaching a plateau. Therefore, both

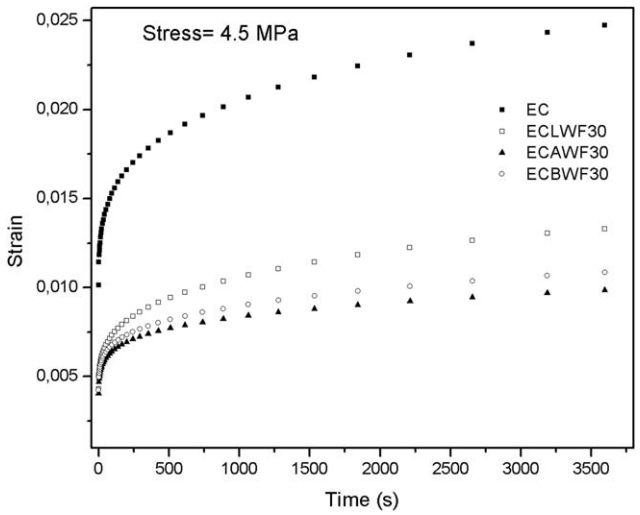

Figure 13. Tensile creep curves at 4.5 MPa of EC and its composites at 30 wt % in wood fibers.

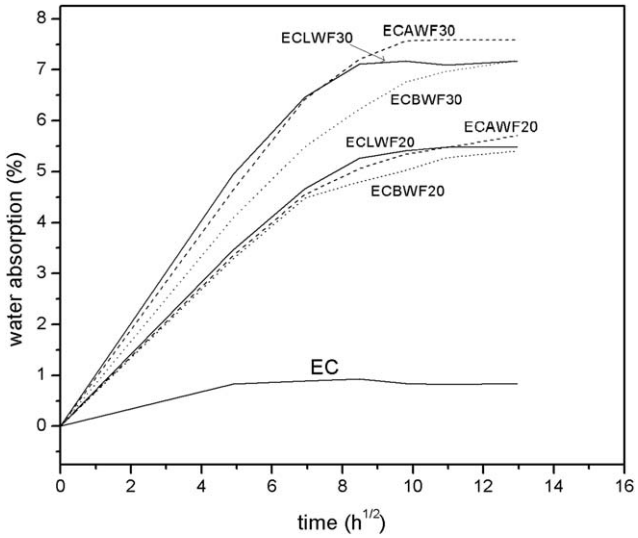

Figure 14. Water uptake versus time1/2, at room temperature for EC and its composites.

matrix and its composites seem to follow a Fickian behavior.[39] The extent of water uptake for the wood composites depends on the amount and the nature of the filler. In this study, it is obvious that Lignocel fibers, which have the largest size and differ at the raw material, resist less at water for both filler loadings. On the contrary, the low fiber size composites (ECBWF20, ECBWF30) seem to absorb less water. Generally, it is expected that shorter fibers would lead to a larger surface area and more OH groups coming from cellulose would be available to absorb water.[18] However, the trend for the specific composites is converse, probably due to the fact that smaller fibers are expected to agglomerate more than larger ones. Another reason for this result may be the void formation during the processing procedure, which in the case of ECBWF seems to be more intense.

To correlate our experimental data with a theoretical model and estimate the diffusivity of the composites, Fick's theory was

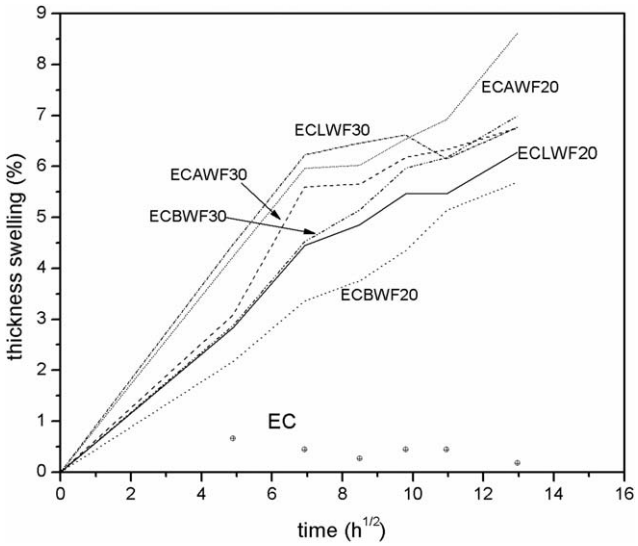

Figure 15. Thickness swelling versus time1/2, during immersion in water at room temperature for EC and its composites.

Table IV. Water Uptake Results

Sample	Saturation moisture uptake M_m (%)	Initial slope of $M_{(t)}$ versus $h^{1/2}$	Diffusion coefficient, D, $\times 10^{-3}$ (mm^2/h)
EC	0.9	0.2	8.5
ECLWF20	5.5	0.7	4.6
ECLWF30	7.2	0.94	5.6
ECAWF20	5.7	0.7	4.5
ECAWF30	7.6	0.9	5.0
ECBWF20	5.4	0.65	4.5
ECBWF30	7.2	0.8	3.6

used. The ability of the solvent molecules to insert to the composite structure is expressed by the diffusion coefficient D.[40] For small times of immersion, eq. (3) can be used:[40]

$$\mathrm{WA} = \frac{4\mathrm{WA}_m}{d}\left(\frac{t}{\pi}\right)^{0.5} D^{0.5} \quad (3)$$

where d is the thickness of the sample (in mm), t is the immersion time (in h) and WA_m is the maximum moisture content (in g) attained. D can be obtained by the initial slope of the curves from Figure 14. The corresponding results are summarized in Table IV. Higher fiber loaded samples seem to contain a greater diffusivity except the ECBWF composites. Concerning the filler type, for WF 20 wt % composites have almost the same value of the diffusion coefficient. At WF 30 wt %, the diffusivity value is clearly affected by the wood fiber size.

CONCLUSIONS

In this study, fully biodegradable wood composites were prepared, by using three different wood flour types at 20 and 30 wt % each. The awaited reinforcing effect that wood fibers will provide, is dependent on the quality of the interfacial adhesion between the matrix and the fibers. In this kind of composites, the compatibility between the two materials depends on the selected matrix, and the type and content of the compatibilizer that will be used. All series of Ecovio/wood flour composites generally revealed enhanced mechanical properties, and low resistance to water uptake. The variety of mechanical properties of the composites examined, renders them promising materials for their use in a wide range of applications. The best improvement in modulus of elasticity was achieved for Arbocel fibers at 30 wt % (ECAWF30, ECBWF30) and Lignocel fibers at 20 wt % (ECLWF20). The highest yield stress was obtained for ECAWF30, followed by ECBWF20 and ECBWF30. A similar trend was obtained by DMA and creep results.

From the above results, it may be extracted that Lignocel composites attain predominant properties at 20 wt %, while cellulose (Arbocel) fibers seem to be suitable for higher weight fractions, providing better mechanical enhancement.

ACKNOWLEDGMENTS

This research has been co-financed by the European Union (European Social Fund, ESF) and Greek national funds through the Operational Program "Education and Lifelong Learning, Research Funding Program Aristeia" (to E.K.).

REFERENCES

1. Nitz, H.; Semke, H.; Landers, R.; Mulhaupt, R. *J. Appl. Polym. Sci.* **2001**, *81*, 1972.
2. Wang, H.; Sun, X.; Seib, P. *J. Appl. Polym. Sci.* **2002**, *84*, 1257.
3. Lee, S. H.; Yoshioka, M.; Shiraishi, N. *J. Appl. Polym. Sci.* **2000**, *77*, 2908.
4. Lee, S. H.; Ohkita, T. *J. Appl. Polym. Sci.* **2003**, *90*, 1900.
5. Yang, H. S.; Yoon, J. S.; Kim, M. N. *Polym. Degrad. Stab.* **2005**, *87*, 131.
6. Pan, P.; Zhu, B.; Kai, W.; Dong, T.; Inoue, Y. *J. Appl. Polym. Sci.* **2008**, *107*, 54.
7. Siegenthaler, K.; Künkel, A.; Skupin, G.; Yamamoto, M. *Adv. Polym. Sci.* **2012**, *245*, 91.
8. Gan, Z.; Kuwabara, K.; Yamamoto, M.; Abe, H.; Doi, Y. *Polym. Degrad. Stab.* **2004**, *83*, 289.
9. Koutsomitopoulou, A. F.; Bénézet, J. C.; Bergeret, A.; Papanicolaou, G. C. *Power Technol.* **2014**, *255*, 10.
10. Kontou, E.; Georgiopoulos, P.; Niaounakis, M. *Polym. Comp.* **2012**, *33*, 282.
11. Georgiopoulos, P.; Kontou, E.; Niaounakis, M. *Polym. Comp.* **2014**, *35*, 1140.
12. Rosa, M. F.; Chiou, B.; Medeiros, E. S.; Wood, D. F.; Mattoso, L. H. C.; Orts, W. J.; Imam, S. H. *J. Appl. Polym. Sci.* **2009**, *111*, 612.
13. Takatani, M.; Ikeda, K.; Sakamoto, K.; Okamoto, T. *J. Wood. Sci.* **2008**, *54*, 54.
14. Qui, W.; Endo, T.; Hirotsu, T. *J. Appl. Polym. Sci.* **2004**, *94*, 1326.
15. Marcovich, N. E.; Reboredo, M. M.; Aranguren, M. I. *J. Appl. Polym. Sci.* **1998**, *70*, 2121.
16. Lee, S. Y.; Kang, I. A.; Doh, G. H.; Yoon, H. G.; Park, B. D.; Wu, O. *J. Thermoplast. Comp. Mater.* **2008**, *21*, 209.
17. Clemons, C. *Forest Product J.* **2002**, *52*, 10.
18. Ichazo, M. N.; Albano, C.; Gonzalez, J.; Perera, R.; Candal, M. V. *Compos. Struct.* **2001**, *54*, 207.
19. Maldas, D.; Kokta, B. V. *J. Adhes. Sci. Technol.* **1998**, *3*, 529.
20. Noel, O.; Clark, R. In 8th International Conference on Wood Fiber-plastic Composites; Madison, WI, May 23–25, 2005.
21. Sykacek, E.; Hrabalova, M.; Frech, H.; Mundigler, N. *Compos. A* **2009**, *40*, 1272.
22. Ludvik, C. N.; Glenn, G. M.; Klamczynski, A. P.; Wood, D. F. *J. Polym. Environ.* **2007**, *15*, 251.
23. Srithep, Y.; Sabo, R.; Clemons, C.; Turng, L. S.; Pilla, S.; Peng, J. In Proceedings of the Polymer Processing Society, 28th Annual Meeting, Pattaya, Thailand, December 11–15, 2012.
24. Tserki, V.; Matzinos, P.; Panayiotou, C. *Compos. A* **2006**, *37*, 1231.

25. Sykacek, E.; Schlager, W.; Mundigler, N. *Polym. Comp.* **2010**, *31*, 443.
26. Morreale, M.; Scaffaro, R.; Maio, A.; La Mantia, F. P. *Compos. A* **2008**, *39*, 503.
27. Detyothin, S.; Selke, S. E. M.; Narayan, R.; Rubino, M.; Rafael Auras, R. *Polym. Degrad. Stab.* **2013**, *98*, 2697.
28. Kontou, E.; Niaounakis, M.; Georgiopoulos, P. *J. Appl. Polym. Sci.* **2011**, *122*, 1519.
29. Pluta, M.; Murariu, M.; Alexandre, M.; Galeski, A.; Dubois, P. *Polym. Degrad. Stab.* **2008**, *93*, 925.
30. Chen, H.; Wang, Y.; Chen, J.; Yang, J.; Zhang, N.; Huang, T.; Wang, Y. *Polym. Degrad. Stab.* **2013**, *98*, 2672.
31. Ren, J.; Fu, H.; Ren, T.; Yuan, W. *Carbohydr. Polym.* **2009**, *77*, 576.
32. Idicula, M.; Boudenne, A.; Umadevi, L.; Ibos, L.; Candau, Y.; Thomas, S. *Comp. Sci. Technol.* **2006**, *66*, 2719.
33. Rozman, H. D.; Tan, K. W.; Kumar, R. N.; Abubakar, A.; Ishak, Z. A. M.; Ismail, H. *Eur. Polym. J.* **2000**, *36*, 1483.
34. Ismail, H.; Hong, H. B.; Ping, C. Y.; Abdul Khalil, H. P. S. *J. Thermoplast. Comp. Mater.* **2003**, *16*, 121.
35. Jouault, N.; Vallat, P.; Dalmas, F.; Said, S.; Jestin, J.; Boué, F. *Macromolecules* **2009**, *42*, 2031.
36. Triebel, C.; Münstedt, H. *Polymer* **2011**, *52*, 1596.
37. Ferry, J. D. In Viscoelastic Properties of Polymers; Ferry, J. D., Ed.; Wiley: New York, **1970**; Chapter *3*, p 303.
38. Osman, M. A.; Atallah, A. *Polymer* **2006**, *47*, 2357.
39. Shen, C. H.; Springer, G. S. *J. Comp. Mater.* **1976**, *10*, 2.
40. Espert, A.; Vilaplana, F.; Karlsson, F. *Compos. A* **2004**, *35*, 1267.